

Manuscript Number:

Title: The cyclic keto-enol insecticide spirotetramat inhibits insect and spider mite acetyl-CoA carboxylases by interfering with the carboxyltransferase partial reaction.

Article Type: Full Length Article

Keywords: Acetyl-CoA carboxylase, insect, spider mite, spirotetramat-enol, insecticide, mode of action, competitive inhibition, carboxyltransferase, mutagenesis

Corresponding Author: Dr. Peter Luemmen, Ph.D.

Corresponding Author's Institution: Bayer CropScience AG

First Author: Peter Luemmen, Ph.D.

Order of Authors: Peter Luemmen, Ph.D.; Jahangir Khajehali, Ph.D.; Kai Luther, B.Sc.; Thomas van Leeuwen, Ph.D.

Abstract: Acetyl-CoA carboxylase (ACC) catalyzes the committed and rate-limiting step in fatty acid biosynthesis. The two partial reactions, carboxylation of biotin followed by carboxyl transfer to the acceptor acetyl-CoA, are performed by two separate domains in animal ACCs. The cyclic keto-enol insecticides and acaricides have been proposed to inhibit insect ACCs. In this communication, we show that the enol derivative of the cyclic keto-enol insecticide spirotetramat inhibited ACCs partially purified from the insect species *Myzus persicae* and *Spodoptera frugiperda*, as well as the spider mite (*Tetranychus urticae*) ACC which was expressed in insect cells using a recombinant baculovirus. Steady-state kinetic analysis revealed competitive inhibition with respect to the carboxyl acceptor, acetyl-CoA, indicating that spirotetramat-enol bound to the carboxyltransferase domain of ACC. Interestingly, inhibition with respect to the biotin carboxylase substrate ATP was uncompetitive, which may indicate that the keto-enol binding site was formed following long-range conformational change triggered by ATP binding. Amino acid residues in the carboxyltransferase domains of plant ACCs are important for binding of established herbicidal inhibitors. Mutating the spider mite ACC at the homologous positions, for example L1736 to either isoleucine or alanine, and A1739 to either valine or serine, did not affect the inhibition of the spider mite ACC by spirotetramat-enol. These results indicated different binding modes of the keto-enols and the herbicidal chemical families.

The cyclic keto-enol insecticide spirotetramat inhibits insect and spider mite acetyl-CoA carboxylases by interfering with the carboxyltransferase partial reaction

Peter Lümmer^{a*}, Jahangir Khajehali^{b,c}, Kai Luther^a, Thomas Van Leeuwen^{b,d}

^aBayerCropScience AG, 40789 Monheim, Germany

^bDepartment of Crop Protection, Faculty of Bioscience Engineering, Ghent University, Ghent, Belgium

^ccurrent address: Department of Plant Protection, College of Agriculture, Isfahan University of Technology, Isfahan, Islamic Republic of Iran

^dInstitute for Biodiversity and Ecosystems Dynamics, University of Amsterdam, Amsterdam, The Netherlands

*Corresponding author: Bayer CropScience AG, Bldg. 6220, Alfred-Nobel-Str. 50, 40789 Monheim, Germany; e-mail: peter.luemmen@bayer.com

Abstract

Acetyl-CoA carboxylase (ACC) catalyzes the committed and rate-limiting step in fatty acid biosynthesis. The two partial reactions, carboxylation of biotin followed by carboxyl transfer to the acceptor acetyl-CoA, are performed by two separate domains in animal ACCs.

The cyclic keto-enol insecticides and acaricides have been proposed to inhibit insect ACCs. In this communication, we show that the enol derivative of the cyclic keto-enol insecticide spirotetramat inhibited ACCs partially purified from the insect species *Myzus persicae* and *Spodoptera frugiperda*, as well as the spider mite (*Tetranychus urticae*) ACC which was expressed in insect cells using a recombinant baculovirus. Steady-state kinetic analysis revealed competitive inhibition with respect to the carboxyl acceptor, acetyl-CoA, indicating that spirotetramat-enol bound to the carboxyltransferase domain of ACC. Interestingly, inhibition with respect to the biotin carboxylase substrate ATP was uncompetitive, which may indicate that the keto-enol binding site was formed following long-range conformational change triggered by ATP binding.

Amino acid residues in the carboxyltransferase domains of plant ACCs are important for binding of established herbicidal inhibitors. Mutating the spider mite ACC at the homologous positions, for example L1736 to either isoleucine or alanine, and A1739 to either valine or serine, did not affect the inhibition of the spider mite ACC by spirotetramat-enol. These results indicated different binding modes of the keto-enols and the herbicidal chemical families.

Keywords

Acetyl-CoA carboxylase, spider mite, spirotetramat-enol, insecticide, mode of action, competitive inhibition, carboxyltransferase, mutagenesis

1. Introduction

Acetyl-coenzyme A carboxylase (ACC, EC 6.4.1.2) catalyzes the first committed and rate-limiting step in the biosynthesis of fatty acids, the carboxylation of acetyl-CoA to malonyl-CoA. Catalysis is biotin-dependent and proceeds through two separate half-reactions, first biotin is carboxylated which is followed by the transfer of the carboxyl group from carboxybiotin to the acyl-CoA acceptor (Fig. 1). In prokaryotes, these half-reactions are performed by distinct protein subunits, whereas eukaryotic ACCs are large, multi-domain enzymes with molecular weights of 265 – 280 kDa. In humans, two genes code for two ACC isoforms, ACC1 and ACC2, with distinct cellular and tissue-specific localization (Tong, 2005). Malonyl-CoA produced by the cytosolic ACC1 is mainly used for fatty acid biosynthesis in lipogenic tissues. ACC2 is associated with mitochondria and is involved in the regulation of the β -oxidation of fatty acids (Tong and Harwood, 2006, Abu-Elheiga et al., 2000). Genomic data suggest that in insects (Parvy et. al., 2012) and mites (Demaeght et al., 2013) single genes code for multidomain ACCs. In the first step, catalyzed by the biotin carboxylase (BC) domain of eukaryotic ACCs, the N1 atom of the biotin cofactor is carboxylated using bicarbonate. This reaction involves the hydrolysis of ATP and leads to the formation of a carboxyphosphate intermediate. Two equivalents of Mg^{2+} are required for the reaction: one Mg^{2+} ion is chelated by the phosphate groups of the nucleotide, the other is bound in the active site.

The second half-reaction is performed by the carboxyltransferase (CT) domain. Carboxybiotin transfers the carboxyl group to the acceptor substrate, acetyl-CoA (Tong, 2005; Waldrop et al., 2012).

Structural data revealed that the active sites of the BC and CT domains of biotin-dependent eukaryotic carboxylases are roughly 55 – 80 Å apart. This means that biotin-mediated carboxyl transfer has to bridge a gap between distant catalytic sites. Biotin is covalently attached to the ϵ -amino group of a lysine residue of the biotin carboxyl carrier protein (BCCP) domain, so that the lysine side chain and the biotin form a highly flexible arm of about 16 Å. The flexible biotin arm together with additional movements of the whole BCCP domain is thought to facilitate the coupling of the two half-reactions, referred to as the 'swinging domain' model (Tong, 2013).

Animal ACCs are regulated by post-translational mechanisms such as phosphorylation and dephosphorylation (Thampy and Wakil, 1985). Allosteric activation by citrate is also well established, although the precise mechanism of citrate activation is not fully understood. Published data suggest that a polymeric state of up to 10 – 20 protomers is induced by citrate (Beatty and Lane, 1982; Tong, 2005) and this supramolecular state is probably essential for full catalytic activity.

In the pharmaceutical area, ACC has been suggested as a therapeutic target for treatment of obesity and cancer due to its central role in fatty acid metabolism (Tong, 2005; Harwood, 2004). In the agrochemical field, three classes of herbicides inhibit the multi-domain ACC isoform in the plastids of grasses (*Poaceae*): the aryloxyphenoxypropionic acids (FOPs), the cyclohexanediones (DIMs) and the phenylpyrazoline compound pinoxaden. Interestingly, plants possess both cytosolic and plastidic ACC isoenzymes. While in dicots the plastidic ACC is a multi-subunit enzyme similar to the prokaryotic forms, only the multi-domain plastidic ACC of grasses is targeted by the herbicides (Powles and Yu, 2010). Resistance mutations as well as X-ray structural evidence revealed that the herbicidal ACC inhibitors bind

to the CT domain. For example, mutation of the Ile1781 residue in the CT domain of black-grass (*Alopecurus myosuroides*) chloroplast ACC caused cross-resistance to the herbicides cycloxydim and clodinafop (Delye et al., 2003). Expression and structural analysis of the yeast ACC CT domain dimer revealed that the herbicide haloxyfop binds at the interface of the CT monomers (Zhang et al., 2003).

The tetrone/tetramic acid family of acaricidal and insecticidal ACC inhibitors, together referred to as cyclic keto-enols, was complemented recently by the spirocyclic tetramic acid derivative, spirotetramat (Fig. 2, A) (Nauen et al., 2003). In contrast to the first commercial keto-enol, spirotetramat controls a broader spectrum of sucking insect species (Bretschneider et al., 2012a). After being taken up into the plant, spirotetramat is readily hydrolyzed to the enol form (Figure 2, B), which has unique systemic properties as it is translocated in the xylem as well as in the phloem of crop plants (Brück et al., 2009).

Based on the fact that cyclic keto-enols were developed from an ACC inhibitor class with herbicidal activity (Bretschneider et al., 2012a), we investigated the mechanism of ACC inhibition by spirotetramat-enol (SPT-enol). For this purpose, we performed enzyme kinetic experiments on partially purified insect and spider mite ACCs. It was assumed that cyclic keto-enols inhibit the CT partial reaction like a lipophilic acyl-CoA mimic similar to the herbicide compounds. However, these are only weak inhibitors of animal ACCs (Tong and Harwood, 2006). Additionally, we report here for the first time the recombinant expression of a catalytically active arthropod ACC.

2. Materials and methods

2.1 Biological material

Spodoptera frugiperda larvae were reared on artificial diet to the L2 stage. Green peach aphids (*Myzus persicae*) were maintained on cabbage plants. Insects were collected, immediately frozen in liquid nitrogen, and stored at -80° C until enzyme preparation.

2.2 Buffers and reagents

Acetyl-CoA, ATP, biotin and buffer reagents were obtained from Sigma-Aldrich, Germany. Spirotetramat-enol was synthesized at Bayer CropScience AG. Sodium [¹⁴C]bicarbonate, specific activity: 2,04 GBq mmol⁻¹, radioactive concentration 74 MBq ml⁻¹ was purchased from Amersham/GE Healthcare. All reagents were of the highest purity available.

2.3 Preparation and partial purification of the aphid ACC

The *M. persicae* ACC was extracted by homogenization of 14 g fresh weight of aphids in 50 ml extraction buffer consisting of 20 mM HEPES, pH 7.5, 150 mM NaCl, 1.0 mM EDTA, 1.0 mM DTT, 10% (v/v) glycerol, and protease inhibitor cocktail Halt™ (Thermo/Pierce) using a Potter-Elvehjem homogenizer at 1000 rpm/10 strokes. The homogenate was filtered through four layers of cheesecloth and centrifuged for 15 min at 3000 g (4° C). The supernatant was filtered again through 4 layers of cheesecloth to remove the lipids and centrifuged for 30 min at 100,000 g (4° C) in a Beckman Coulter 45Ti rotor. The supernatant

was again filtered through cheesecloth and loaded on an anion exchange chromatography column (HiLoad Q-Sepharose FastFlow 26/10, GE Healthcare). Elution of bound proteins was performed with a linear NaCl gradient from 250 mM to 1 M at a flow rate of 2.0 ml min⁻¹. Fractions of 8 ml were collected and tested for ACC activity. Active fractions were pooled and subjected to buffer exchange on PD-10 gel filtration columns (GE Healthcare) equilibrated with HKM buffer (100 mM HEPES, pH 7.5, 15 mM potassium citrate, 15 mM MgCl₂ hexahydrate). Protein concentrations were determined by the method of Bradford (Bradford, 1976). Before storage at -80° C, 10% (v/v) glycerol was added to the enzyme solution.

2.4 Preparation and partial purification of *Spodoptera frugiperda* ACC

8 g of *Spodoptera* larvae were homogenized in 32 ml extraction buffer and a cleared extract was prepared by differential centrifugation. Anion exchange chromatography was applied for partial purification essentially as described above for the *Myzus* enzyme (2.3).

2.5 Construction of recombinant baculoviruses

The ACC full length sequence of *T. urticae* (tetur21g02170, GenBank accession numbers KC513765, KC513766, KC513767) (Demaeght et al., 2013) was cloned from cDNA by nested PCR using primer pairs TurACCuntF3/R3 designed in UTR regions and TurACCF3a/ TurACCuntR2 (from start to 5'UTR) in the second reaction. This PCR product was ligated into the CloneJET™ vector and sequenced as previously described (Demaeght et al., 2013). Using a correct clone (pJetACCF3) as template, a PCR was performed using primers TurACC-ExpF1/ TurACC-ExpR1 to introduce the restriction site for NotI and XbaI and delete the initiation codon. This PCR product was blunted and ligated into the CloneJET™ vector and re-sequenced. A correct clone was triple digested (NotI, XbaI and BglI) and ligated in frame into the digested (NotI and XbaI) vector pFastBac HT C, downstream the polyhedron promoter. Colony PCR with primers pFastBac HT-F/R identified positive pFastBac clones. A correct plasmid (pFast HTC12) was recombined into the bacmid backbone following the recommendations of the Bac-to-Bac® Baculovirus Expression system (Invitrogen, USA). Colonies containing the recombinant bacmid were identified as white on Luria Bertani (LB) plates in the presence of blue-gal, isopropyl-L-thio-β-D-galactoside, and antibiotics (kanamycin, gentamicin, and tetracycline). Recombinant bacmids were purified from bacterial cells by classical plasmid preparation protocols using the alkaline lysis method (Birnboim and Doly, 1979) and analyzed by PCR using primers pUC/M13F and pUC/M13R to verify the presence and site of insertion of ACC in the bacmids. Primer sequences are listed in Table 1.

For the recombinant production of ACC proteins with AA replacements L1736I, L1736A, A1739V and A1739S, the pFastHTC12 plasmid was mutated by Genscript (US) and codon changes CTT to ATC, CTT to GCT, GCT to GTC and GCT to TCC were introduced respectively. Mutated plasmids were re-sequenced to verify sequence changes (See also Figure 7).

Bacmids were transfected into Sf9 cells using Cellfectin II, essentially following the manufacturer's protocol (Invitrogen/Life Technologies). Recombinant baculoviruses were selected in standard plaque

assays and high-titer virus stocks were generated after infection of Sf9 cells grown in serum-free medium (Sf-900™ II SFM, Life Technologies).

2.6 Expression of *Tetranychus urticae* ACC

Trichoplusia ni cells (BTI-TN-5B1-4, High Five™, Invitrogen/Life Technologies) cultured in ExpressFive™ serum-free medium (Invitrogen/Life Technologies) were used for expression of the *T. urticae* ACC. HighFive cells were grown in suspension culture volumes of 50 ml in 250 ml-flasks at 27°C under agitation. Cells were infected at a cell density of about $0.5 \cdot 10^6$ /ml with the baculovirus Bac4_TetACC at a multiplicity of infection of 1.0. At 48 h post infection, cells were harvested by centrifugation and washed with phosphate-buffered saline. Cell pellets were suspended in 4 volumes (relative to cell pellet volumes) of 10 mM HEPES, pH 7.4, 20 mM KCl, 15 mM potassium citrate, 0.1 mM DTT, and the protease inhibitor cocktail Halt™ (Thermo/Pierce) at 4°C and lysed by sonication (5 x 20 s, 70% power output) on ice with cooling between the sonication cycles. Cellular debris and membranes were centrifuged for 20 min at 13,000 x g. The supernatant was used as a crude enzyme preparation and tested for ACC activity and subjected to anion exchange chromatography essentially as described above for the *Myzus* enzyme (2.3).

2.7 ACC activity assay

The ACC activity assay measured the carboxylation of acetyl-CoA using sodium [¹⁴C]bicarbonate to form [¹⁴C]malonyl-CoA as described previously with minor modifications (Beatty and Lane, 1982, Goldring and Read, 1994). The reaction mix of 200 µl contained 20 µg partially purified ACC in 100 mM HEPES, pH 7.5, 15 mM MgCl₂ hexahydrate, 15 mM potassium citrate, 100 µg/ml BSA. The final concentrations of ATP and acetyl-CoA were 4 mM and 1 mM, respectively. The reaction was started 2.5 mM sodium bicarbonate containing 9 µM sodium [¹⁴C]bicarbonate as a tracer. Following 30 min incubation at 25°C, the reaction was acidified with 35 µl 6N HCl and agitated for 10 min to convert the acid-labile bicarbonate into carbon dioxide and outgassing the unreacted [¹⁴C]O₂. The amount of [¹⁴C]malonyl-CoA formed during the reaction was determined by liquid scintillation counting. Appropriate controls without protein and without acetyl-CoA were performed to correct for traces of unreacted bicarbonate or [¹⁴C]-labeled side products.

For ACC inhibition measurements, variable concentrations of inhibitors (dissolved in DMSO, 2% v/v final concentration) were added to the reactions mixtures; the controls received pure DMSO. Data evaluation and the calculation of kinetic parameters were performed with SigmaPlot 11 (SYSTAT). Inhibitor constants, K_i, were calculated according to Cheng and Prusoff (Cheng and Prusoff, 1973).

3. Results

3.1 Partial purification and initial enzymatic characterization of insect and spider-mite ACCs

Soluble protein extracts from either mixed populations of *M. persicae*, L4 larvae of *S. frugiperda*, or baculovirus-infected HighFive cells expressing the *T. urticae* ACC were partially purified from the centrifuged crude extracts by anion exchange chromatography on Q-Sepharose. The specific activities could be enriched about hundred fold by this step. Addition of citrate was always found to be essential for

full enzymatic activity and provided reasonable stability during storage at -80°C of all three arthropod ACCs described.

Specific activities of the partially purified ACC preparations were 7.9 mU mg^{-1} for the *S. frugiperda* ACC, 8.5 mU mg^{-1} for the *M. persicae* enzyme, and 18.5 mU mg^{-1} for the recombinantly expressed *T. urticae* ACC. Steady-state kinetics of the total ACC reaction as measured by malonyl-CoA formation followed simple Michaelis-Menten type kinetics, when the CT domain substrate acetyl-CoA concentration was varied (Figure 3). The apparent K_m values were calculated by fitting the data to the Michaelis-Menten equation and revealed $290\text{ }\mu\text{M}$ (*S. frugiperda*), $370\text{ }\mu\text{M}$ (*M. persicae*), and $350\text{ }\mu\text{M}$ (*T. urticae*). Similar steady-state kinetics were obtained for all three ACC enzymes tested when the BC substrate ATP was varied: typical K_m values for ATP ranged between 160 and $220\text{ }\mu\text{M}$.

3.2 Arthropod ACC inhibition by spirotetramat-enol

Spirotetramat-enol is the hydrolysis product of the keto-enol insecticide spirotetramat. In this study, SPT-enol was found to be a potent inhibitor of three different arthropod ACCs partially purified from *S. frugiperda*, *M. persicae*, and *T. urticae* (Figure 4). The characteristic sigmoidal dose-response curves revealed similar SPT-enol concentrations causing 50% inhibition of ACC activities (IC_{50} values): 102 nM for the *Spodoptera* enzyme, 126 nM for the aphid ACC, and 123 nM for the spider mite enzyme. Inhibitor constants, K_i , of SPT-enol for the three enzymes were derived from the Cheng-Prusoff equation, $K_i = \text{IC}_{50}/(1 + [s]/K_m)$, using the substrate concentration, $[s]$ of 1.0 mM and the K_m values determined from Figure 3 (3.1). The calculated K_i values were 23 nM (*S. frugiperda*), 34 nM (*M. persicae*), and 32 nM (*T. urticae*).

3.3 Steady-state kinetics of arthropod ACC inhibition by spirotetramat-enol

Insect biological starting material provided ample yields of partially purified ACCs to elucidate the inhibitory mechanism of SPT-enol by steady-state kinetic analysis. ACC activities plotted against variable concentrations of the carboxyltransferase substrate acetyl-CoA showed a pronounced increase in the apparent K_m values from 0.3 mM (control) to 1.14 mM in the presence of 300 nM SPT-enol (Fig 5A). The apparent maximum enzyme activities, V_{max} , did not differ substantially in the range of 5.8 to 6.8 mU mg^{-1} . Double-reciprocal plots (Fig. 5B) illustrated a competitive interaction of the inhibitor with the binding of the CT substrate as characterized by a common intersection point on the y-axis (V_{max}^{-1}).

Essentially the same results were obtained with the *Tetranychus* ACC. SPT-enol at 300 nM concentration increased the apparent K_m from 0.35 to 1.3 mM , whereas the V_{max} values were 18.5 mU mg^{-1} for the absence, and 17.8 mU mg^{-1} in the presence of SPT-enol (data not shown).

Interestingly, measuring ACC inhibition of SPT-enol at variable ATP substrate concentrations revealed that the inhibitor (300 nM) slightly decreased the apparent K_m , i.e. increased the affinity for ATP from 0.22 mM to 0.14 mM . The effect on the maximum initial velocity, V_{max} , of the total reaction was even more pronounced: the apparent specific activity was decreased from 18.4 mU mg^{-1} to 8.5 mU mg^{-1} in the

presence of 300 nM SPT-enol (Fig. 6A). Double-reciprocal plots resulted in parallel regression lines that are characteristic of uncompetitive inhibition with respect to the BC substrate, ATP (Fig. 6B).

3.4 Mutations in the CT domain of *Tetranychus urticae* ACC

Mutations into the putative DIM/FOP inhibitor binding site of the *Tetranychus* ACC cDNA were introduced at two positions. The first position at AA 1736 corresponds to the conserved I1781 in the plant plastid ACC (*A. myosuroides* numbering) and a I1781L substitution has been frequently associated with FOPs and DIMs target-site resistance in a number of grass weeds (Figure 7). In the mite protein, a leucine is present at this position, and we introduced the L1736I and L1736A substitutions to assess the effect on mite enzyme catalytic activity and inhibitor sensitivity (Figure 7). The second position is A1739 (corresponding to the conserved S1783 in monocotyledonous and dicotyledonous plants) which is located in the deep binding pocket (Zhang et al., 2004). The substitutions A1739S and A1739V were introduced (Fig. 7).

The specific ACC activities of both L1736 mutants were reduced (Fig. 8). Replacement of leucine1778 by isoleucine led to a reduction of about 27% as compared to the wild-type. A more severe effect was observed, when L1736 was replaced by alanine, showing only about 40% of the wild-type ACC activity. Mutation of the second position, alanine 1739, to serine did not have a measurable effect on the catalytic performance. However, ACC activity was reduced by about 50% when A1739 was replaced by valine. All of the CT mutants were fully sensitive to inhibition by SPT-enol at 300 nM.

4. Discussion

Acetyl-CoA carboxylase, EC 6.4.1.2, catalyzes the committed and rate-limiting step in fatty acid biosynthesis. It is a well-established molecular target site for commercially successful herbicides, including the aryloxyphenoxypropionates (FOPs), the cyclohexanediones (DIMs), and the more recently introduced pinoxaden (Devine, 2002, Wenger et al., 2012). Localization of herbicide-resistant mutations as well as structural studies have shown that the herbicidal ACC inhibitor classes bind to the carboxyltransferase (CT) domain of the multidomain ACC isoform in the plastids of grasses (Yu et al., 2007; Liu et al., 2007; Kaundun et al., 2013; Yu et al., 2010).

A novel structural class of acaricides and insecticides, referred to as cyclic keto-enols and represented by the spirocyclic tetronic acid derivatives spirodiclofen and spiromesifen, and the spirocyclic tetramic acid derivative, spirotetramat, have been proposed as ACC inhibitors (Bretschneider et al., 2012a; Bretschneider et al., 2012b), but a detailed biochemical analysis of their inhibitory mechanism has not been reported so far. In accordance with ACC inhibition as the molecular mode of action of cyclic keto-enols, an ACC point mutation replacing the conserved glutamic acid residue at position 645 with lysine was reported to be correlated with spiromesifen resistance in the greenhouse whitefly, *Trialeurodes vaporariorum* (Karatolos et al., 2012).

In this study, we demonstrate the interaction of the enol derivative of spirotetramat (SPT) with insect and spider mite ACCs. After uptake of SPT into the plants, it is rapidly converted to the SPT-enol (Fig. 2),

which accounts for the unique two-way systemic efficacy against diverse species of aphids (Bretschneider et al., 2012a).

Initial attempts to characterize the enzyme by determination of ACC activity in crude extracts of *S. frugiperda* larvae or *M. persicae* with the radioactive carbon dioxide incorporation assay revealed a substantial fraction of acid-resistant radioactivity formed in controls lacking acetyl-CoA and also in the presence of micromolar concentrations of SPT-enol (data not shown). This fraction may be the result of non-specific side reactions unlikely to be catalyzed by ACC. For this reason, we always purified the ACCs by anion exchange chromatography to obtain enzyme preparations that were found to be fully inhibited by the cyclic keto-enols. These preparations were used for subsequent steady-state kinetic analysis in this study. The limitation of biological starting material from spider mites motivated the cloning of the full-length *Tetranychus* ACC and subsequent baculovirus-mediated expression in BTI-TN-5B1-4 insect cells, which delivered reasonably good yields of the catalytically active spider mite enzyme.

The affinities of the two insect and the spider mite ACCs for the CT substrate acetyl-CoA were similar and comparable to those obtained for partially purified ACC from maize suspension cell cultures and other plant sources (Egin-Buhler and Ebel, 1983; Burton et al., 1991; Charles and Cherry, 1986), but considerably higher (factor ~10) than those reported for vertebrate ACCs (Trumble et al., 1995; Beaty and Lane, 1982). The reason for these divergences is not known, but they may result from different states of enzyme purity and/or (allosteric) activation.

All three enzyme preparations were found to be equally sensitive to SPT-enol as demonstrated by the inhibitor constants ranging from 23 – 34 nM.

Given that the structures of ACCs are complex in general, and that the two partial reactions are catalyzed by separate protein domains, it can be presumed that compounds can potentially inhibit different catalytic steps and/or interact with different binding sites. The herbicidal FOPs, DIMs and phenylpyrazolines all bind to the CT domain (Delye et al., 2005; Kaundun, 2010; Yu et al., 2010). However, the myxobacterial polyketide soraphen A was reported as a nanomolar inhibitor of the biotin carboxylase (BC) domains of fungal ACCs (Weatherly et al., 2004), probably by interfering with BC dimerization (Tong, 2013). Finally, a novel class of bispiperidylcarboxamide CT domain inhibitors of mammalian ACCs was discovered by high-throughput biochemical screening (Corbett et al., 2010). Interestingly, X-ray structural data demonstrated different binding positions within the CT domain for the bispiperidylcarboxamide CP-640186 and the herbicide haloxyfop (Zhang et al., 2004).

Steady-state kinetic analysis (Fig. 5) revealed that SPT-enol inhibited the ACC reaction competitively with respect to the CT substrate, acetyl-CoA. This was illustrated by the common intersection point, $1/V_{max}$, of the linear regression lines in double-reciprocal plots (Figure 5, B). Consequently, SPT-enol and acetyl-CoA are likely to bind to at least overlapping sites in the CT domain, which was in line with our working hypothesis.

Although the herbicides sethoxydim and haloxyfop were originally reported as noncompetitive inhibitors with respect to all three ACC substrates under steady-state kinetic conditions (Burton et al., 1991), later X-ray structural analysis of haloxyfop binding to the isolated yeast CT domain revealed that the herbicide

sterically interfered with binding of the substrate's acyl moiety. Furthermore, kinetic analysis showed that haloxyfop inhibited malonyl-CoA binding competitively (Zhang et al., 2003; Tong, 2005).

The bispiperidylcarboxamide compound CP-610431 was shown to inhibit mammalian ACCs non-competitively with respect to acetyl-CoA, bicarbonate and citrate (Harwood et al., 2003).

The steady-state kinetic data were interpreted as distinct binding sites for the known ACC inhibitor classes within the CT domain, a concept that was later substantiated by X-ray structural analysis (Harwood et al., 2003, Zhang et al., 2004). In the context of this discussion, the binding mode of SPT-enol may be similar, but not identical to the aryloxyphenoxypropionates and cyclohexanediones. Distinct orientations of inhibitor binding can plausibly explain the weak affinity of the herbicides to insect and spider mite ACCs (data not shown).

Interestingly, steady-state kinetics of SPR-enol revealed an uncompetitive mode of inhibition with respect to ATP, which is hydrolyzed to form the carboxyphosphate intermediate in the BC partial reaction (Fig. 6, B). The data suggest that the SPT-enol binds exclusively to the enzyme-substrate (ES) complex in contrast to noncompetitive inhibition interpreted as inhibitor binding to the ES complex as well as to the free enzyme. Uncompetitive inhibition is rarely found in monosubstrate reactions, but more often in enzymes performing bi- or multisubstrate reactions. Examples are substrate phosphorylations catalyzed by kinases (VanScyoc et al., 2008; Agnew and Timson, 2010), and the inhibition of phosphoribosyltransferase by histidine (Pedreño et al., 2012). Hypothetically, uncompetitive ACC inhibition by SPT-enol with respect to ATP may indicate that the formation of the keto-enol binding site would require conformational changes in the CT domain. These may be triggered by the BC half-reaction and the concomitant conformational movement of the biotinyl carboxyl carrier (BCC) domain. Accordingly, conformational changes of the binding site located at the interface of the CT dimer have already been implicated in the binding of the herbicidal ACC inhibitors (Tong, 2013).

Furthermore, the assumption of long-range conformational changes essential for inhibitor binding could provide an explanation for a recently identified ACC mutation conferring resistance to the cyclic keto-enol spiromesifen in the greenhouse whitefly, *Trialeurodes vaporariorum* (Karatolos et al., 2012). Unexpectedly, the mutation was not localized in the CT domain, but rather to a position between the BC and the BCC domains of the whitefly ACC. A highly conserved glutamate residue was changed to lysine. This may affect the interaction between the catalytic domains and thus prevent the formation of the high-affinity binding site for the keto-enol. It would be interesting to test this hypothesis by measuring the steady-state kinetics of the mutated whitefly enzyme. Unfortunately, the residue reported in the white fly enzyme is not conserved between insects and mites (Demaeght et al. 2013) and consequently the *in vitro* mutagenesis system based on *T. urticae* ACCase presented in this study could not be used to assess the effect of the whitefly mutation on inhibitor binding.

Several point mutations in the CT domain of ACCs have been reported to confer FOP and/or DIM resistance in grass weeds. In the black-grass, *A. myosuroides*, for example, an isoleucine to leucine substitution at position 1781 reduced the sensitivity to some, but not all FOPs and DIMs (Delye et al., 2004). Interestingly, the homologous position of Ile1781 in *Drosophila* and in *Tetranychus* is leucine, which

may at least partly explain the lack of inhibitor potency of FOPs and DIMs against insect and spider mite ACCs.

Mutation of this position in the spider mite enzyme to either isoleucine or alanine reduced the specific activity of the mutated ACCs indicating that even subtle changes at this position influence the catalytic performance, for example by affecting substrate binding (Figure 8). Substituting the neighboring alanine1781 by valine had a similar effect on activity, whereas a serine in this position had no observable effect on catalysis. Interestingly, SPT-enol was equally potent against the mutant enzymes as compared to the wild-type, indicating that these residues are probably not involved in SPT-enol binding. These preliminary results are in accordance with the hypothesis that keto-enols and the classical CT domain inhibitors are not identical with respect to their binding modes. In view of resistance management, binding site heterogeneity leaves the chance for novel CT inhibitor chemistries with different binding modes to overcome potential target site resistances.

In summary, we have shown that spirotetramat-enol inhibits insect and spider mite ACCs by interacting with the carboxyltransferase domain. The binding modes of SPT-enol and the herbicidal ACC inhibitors are likely different. Systematic mutagenesis of residues in the CT domain should provide further insight into the binding site and the mechanistic details of the keto-enol inhibitors.

Acknowledgements

The excellent technical assistance of Claudia Wehr and Gabi Lachner is gratefully acknowledged.

References

- Abu-Elheiga, L., Brinkley, W.R., Zhong, L., Chirala, S.S., Woldegiorgis, G., Wakil, S.J., 2000. The subcellular localization of acetyl-CoA carboxylase 2. *Proc.Natl.Acad.Sci.USA* 97, 1444-1449.
- Agnew, A., Timson, D., 2010. Mechanistic studies on human N-acetylgalactosamine kinase. *J.Enzyme Inhib.Med.Chem*, 25, 370-376.
- Beaty, N.B., Lane, M.D., 1982. Acetyl coenzyme A carboxylase. Rapid purification of the chick liver enzyme and steady state kinetic analysis of the carboxylase-catalyzed reaction. *J. Biol.Chem.* 257, 924-929.
- Birnboim, H.C., Doly, J., 1979. A rapid alkaline extraction procedure for screening recombinant plasmid DNA. *Nucl.Acids Res.* 7, 1513-1523.
- Bradford, M.M., 1976. A rapid and sensitive method for the quantitation of microgram quantities of protein utilizing the principle of protein-dye binding. *Anal.Biochem.* 72, 248-254.
- Bretschneider, T., Fischer, R., Nauen, R., 2012a. Inhibitors of lipid synthesis: acetyl-CoA-carboxylase inhibitors, in: Krämer, W., Schirmer, U., Jeschke, P., Witschel, M. (Eds.), *Modern Crop Protection Compounds*, 2nd Edition, Wiley VCH, Weinheim, pp. 1108-1126.
- Bretschneider, T., Fischer, R., Nauen, R., 2012b. Tetrionic acid insecticides and acaricides inhibiting acetyl-CoA carboxylase, in: Lamberth, C., Dinges, J. (Eds.), *Bioactive Heterocyclic Compound Classes: Agrochemicals*, Wiley VCH, Weinheim, pp. 265-278.
- Brück, E., Elbert, A., Fischer, R., Krueger, S., Kühnhold, J., Klueken, A.M., Nauen, R., Niebes, J.-F., Reckmann, U., Schnorbach, H.-J., Steffens, R. & Van Waetermeulen, X., 2009. Movento[®], an innovative ambimobile insecticide for sucking insect pest control in agriculture: Biological profile and field performance. *Crop Prot.* 28, 838-844.
- Burton, J.D., Gronwald, J.W., Keith, R.A., Somers, D.A., Gengenbach, B.G., Wyse, D.L., 1991. Kinetics of inhibition of acetyl-coenzyme A carboxylase by sethoxydim and haloxyfop. *Pestic.Biochem.Physiol.* 39, 100-109.
- Charles, D.J., Cherry, J.H., 1986. Purification and characterization of acetyl-CoA carboxylase from developing soybean seeds. *Phytochemistry* 25, 1067-1071.
- Cheng, Y., Prusoff, W.H., 1973. Relationship between the inhibition constant (K_I) and the concentration of inhibitor which causes 50 per cent inhibition (I₅₀) of an enzymatic reaction. *Biochem.Pharmacol.* 22, 3099-3108.
- Corbett, J.W., Freeman-Cook, K.D., Elliott, R., Vajdos, F., Rajamohan, F., Kohls, D., Marr, E., Zhang, H., Tong, L., Tu, M., Murdande, S., Doran, S.D., Houser, J.A., Song, W., Jones, C.J., Coffey, S.B., Buzon, L., Minich, M.L., Dirico, K.J., Tapley, S., McPherson, K.R., Sugarman, E., Harwood, H.J., JR., Esler, W., 2010. Discovery of small molecule isozyme non-specific inhibitors of mammalian acetyl-CoA carboxylase 1 and 2. *Bioorg.Med.Chem.Lett.* 20, 2383-2388.

Delye, C., Straub, C., Matejcek, A., Michel, S., 2004. Multiple origins for black-grass (*Alopecurus myosuroides*, Huds.) target-site-based resistance to herbicides inhibiting acetyl-CoA carboxylase. *Pest Manage.Sci.* 60, 35-41.

Delye, C., Zhang, X.Q., Chalopin, C., Michel, S., POWLES, S.B., 2003. An isoleucine residue within the carboxyl-transferase domain of multidomain acetyl-coenzyme A carboxylase is a major determinant of sensitivity to aryloxyphenoxypropionate but not to cyclohexanedione inhibitors. *Plant Physiol.* 132, 1716-1723.

Delye, C., Zhang, X.Q., Michel, S., Matejcek, A., Powles, S.B., 2005. Molecular bases for sensitivity to acetyl-coenzyme A carboxylase inhibitors in black-grass. *Plant Physiol.* 137, 794-806.

Demaeght, P., Dermauw, W., Tsakireli, D., Khajehali, J., Nauen, R., Tirry, L., Vontas, J., Lümmer, P., Van Leeuwen, T., 2013. Molecular analysis of resistance to acaricidal spirocyclic tetrone acids in *Tetranychus urticae*: CYP392E10 metabolizes spirodiclofen, but not its corresponding enol. *Insect Biochem.Mol.Biol.* 43, 544-554.

Devine, M.D., 2002. Acetyl-CoA carboxylase inhibitors, in: Böger, P., Wakabayashi, K., Hirai, K. (Eds.), *Herbicide Classes in Development, Mode of Action, Targets, Genetic Engineering, Chemistry*, Springer, Heidelberg, New York, pp. 103-113.

Egin-Bühler, B., Ebel, J., 1983. Improved purification and further characterization of acetyl-CoA carboxylase from cultured cells of parsley (*Petroselinum hortense*). *Eur.J.Biochem.* 133, 335-339.

Goldring, J.P., Read, J.S., 1994. Insect acetyl-CoA carboxylase: enzyme activity during adult development and after feeding in the tsetse fly, *Glossina morsitans*. *Comp.Biochem.Physiol.Biochem.Mol.Biol.* 108, 27-33.

Harwood, H.J., Jr., 2004. Acetyl-CoA carboxylase inhibition for the treatment of metabolic syndrome. *Curr.Opin.Investig.Drugs* 5, 283-289.

Harwood, H.J., Jr., Petras, S.F., Shelly, L.D., Zaccaro, L.M., Perry, D.A., Makowski, M.R., Hargrove, D.M., Martin, K.A., Tracey, W.R., Chapman, J.G., Magee, W.P., Dalvie, D.K., Soliman, V.F., Martin, W.H., Mularski, C.J., Eisenbeis, S. A., 2003. Isozyme-nonspecific N-substituted bipiperidylcarboxamide acetyl-CoA carboxylase inhibitors reduce tissue malonyl-CoA concentrations, inhibit fatty acid synthesis, and increase fatty acid oxidation in cultured cells and in experimental animals. *J.Biol.Chem.* 278, 37099-37111.

Karatolos, N., Williamson, M.S., Denholm, I., Gorman, K., French-Constant, R., Nauen, R., 2012. Resistance to spiromesifen in *Trialeurodes vaporariorum* is associated with a single amino acid replacement in its target enzyme acetyl-coenzyme A carboxylase. *Insect Mol.Biol.* 21, 327-334.

Kaundun, S.S., 2010. An aspartate to glycine change in the carboxyl transferase domain of acetyl CoA carboxylase and non-target-site mechanism(s) confer resistance to ACCase inhibitor herbicides in a *Lolium multiflorum* population. *Pest Manage.Sci.* 66, 1249-1256.

Kaundun, S.S., Hutchings, S.-J., Dale, R.P., McIndoe, E., 2013. Role of a novel I1781T mutation and other mechanisms in conferring resistance to acetyl-CoA carboxylase inhibiting herbicides in a black-grass population. *PLoS One* 8, e69568.

Liu, W., Harrison, D.K., Chalupska, D., Gornicki, P., O'Donnell, C.C., Adkins, S.W., Haselkorn, R., Williams, R.R., 2007. Single-site mutations in the carboxyltransferase domain of plastid acetyl-CoA carboxylase confer resistance to grass-specific herbicides. *Proc.Natl.Acad.Sci.USA* 104, 3627-3632.

Nauen, R., Bretschneider, T., Elbert, A., Fischer, R., Tiemann, R., 2003. Spirodiclofen and spiromesifen. *Pestic.Outlook* 14, 243-246.

Parvy, J.P., Napal, L., Rubin, T., Poidevin, M., Perrin, L., Wicker-Thomas, C., Montagne, J., 2012. *Drosophila melanogaster* acetyl-CoA-carboxylase sustains a fatty acid-dependent remote signal to waterproof the respiratory system. *PLoS Genet.* 8, e1002925.

Pedreno, S., Pisco, J.P., Larrouy-Maumus, G., Kelly, G., De Carvalho, L.P.S., 2012. Mechanism of feedback allosteric inhibition of ATP phosphoribosyltransferase. *Biochemistry* 51, 8027-8038.

Thampy, K.G., Wakil, S.J., 1985. Activation of acetyl-CoA carboxylase. Purification and properties of a Mn^{2+} -dependent phosphatase. *J.Biol.Chem.* 260, 6318-6323.

Tong, L., 2005. Acetyl-coenzyme A carboxylase: crucial metabolic enzyme and attractive target for drug discovery. *Cell.Mol.Life Sci.* 62, 1784-1803.

Tong, L., 2013. Structure and function of biotin-dependent carboxylases. *Cell.Mol.Life Sci.* 70, 863-891.

Tong, L., Harwood, H.J., Jr., 2006. Acetyl-coenzyme A carboxylases: Versatile targets for drug discovery. *J.Cell.Biochem.* 99, 1476-1488.

Trumble, G.E., Smith, M.A., Winder, W.W., 1995. Purification and characterization of rat skeletal muscle acetyl-CoA carboxylase. *Eur.J.Biochem.* 231, 192-198.

Vanscyoc, W.S., Holdgate, G.A., Sullivan, J.E., Ward, W.H.J., 2008. Enzyme kinetics and binding studies on inhibitors of MEK protein kinase. *Biochemistry* 47, 5017-5027.

Waldrop, G.L., Holden, H.M., St Maurice, M., 2012. The enzymes of biotin dependent CO₂ metabolism: What structures reveal about their reaction mechanisms. *Protein Sci.* 21, 1597-1619.

Weatherly, S.C., Volrath, S.L., Elich, T.D., 2004. Expression and characterization of recombinant fungal acetyl-CoA carboxylase and isolation of a sorafenib-binding domain. *Biochem.J.* 380, 105-110.

Wenger, J., Niderman, T., Mathews, C.E., 2012. Acetyl-CoA carboxylase inhibitors, in: Krämer, W., Schirmer, U., Jeschke, P., Witschel, M. (Eds.), *Modern Crop Protection Compounds*, 2nd Edition, Wiley VCH, Weinheim, pp. 447-477.

Yu, L.P.C., Kim, Y.S., Tong, L., 2010. Mechanism for the inhibition of the carboxyltransferase domain of acetyl-coenzyme A carboxylase by pinoxaden. *Proc.Natl.Acad.Sci.US*, 107, 22072-22077.

Yu, Q., Collavo, A., Zheng, M.Q., Owen, M., Sattin, M., Powles, S.B., 2007. Diversity of acetyl-coenzyme A carboxylase mutations in resistant *Lolium* populations: evaluation using clethodim. *Plant Physiol.* 145, 547-558.

Zhang, H., Tweel, B., Li, J., Tong, L., 2004. Crystal structure of the carboxyltransferase domain of acetyl-coenzyme A carboxylase in complex with CP-640186. *Structure* 12, 1683-1691.

Zhang, H., Yang, Z., Shen, Y., Tong, L., 2003. Crystal structure of the carboxyltransferase domain of acetyl-coenzyme A carboxylase. *Science* 299, 2064-2067.

Figures

Fig. 1

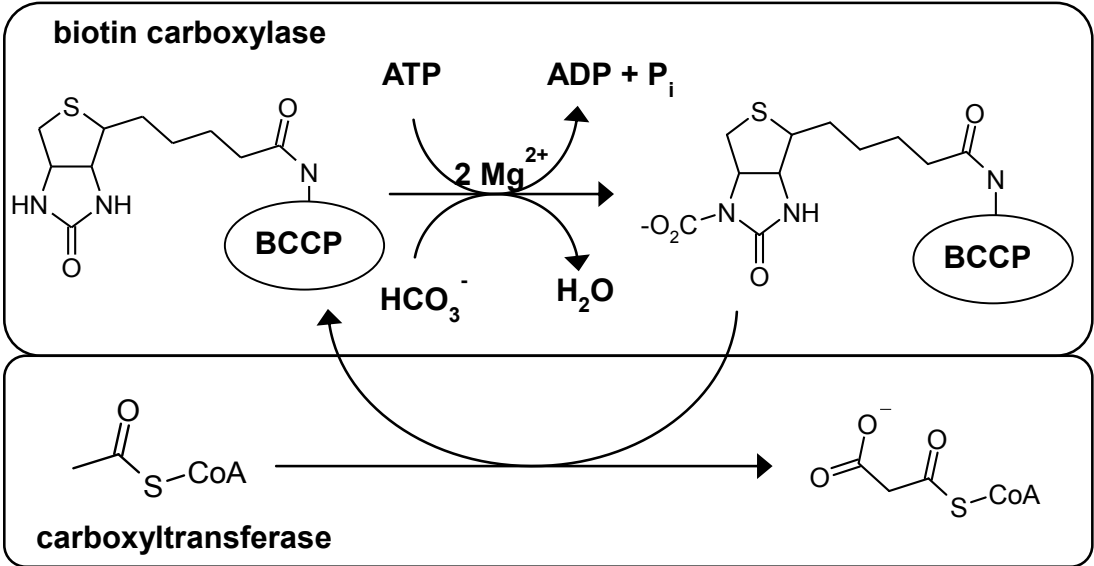


Fig. 2

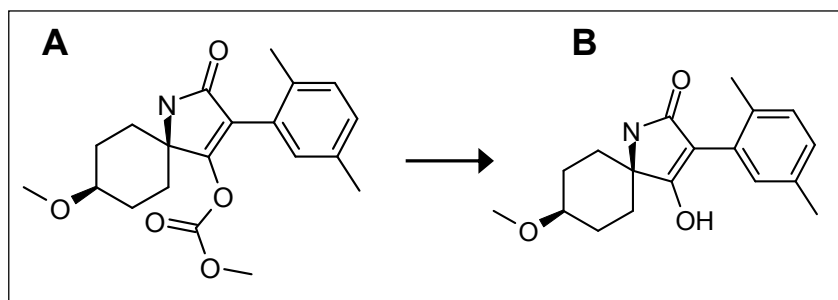


Fig. 3

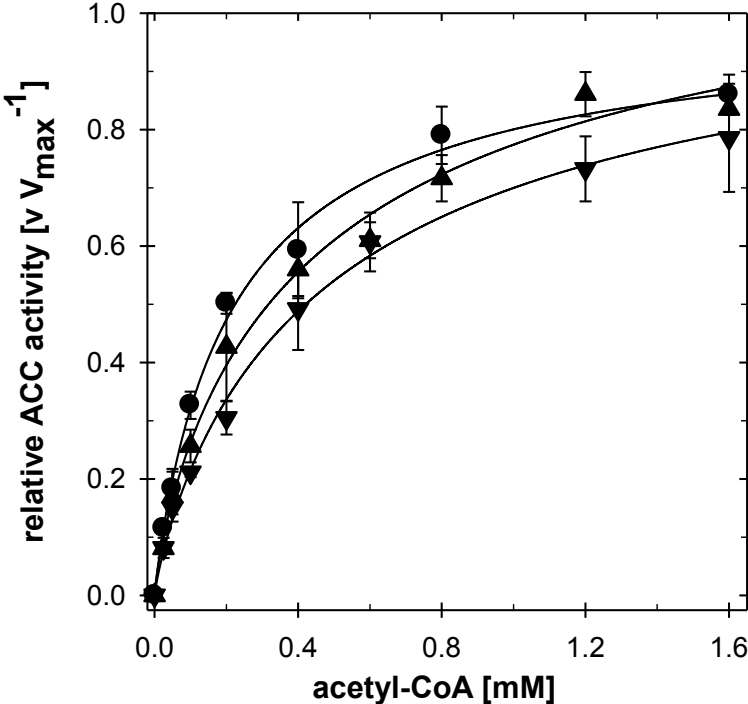


Fig. 4

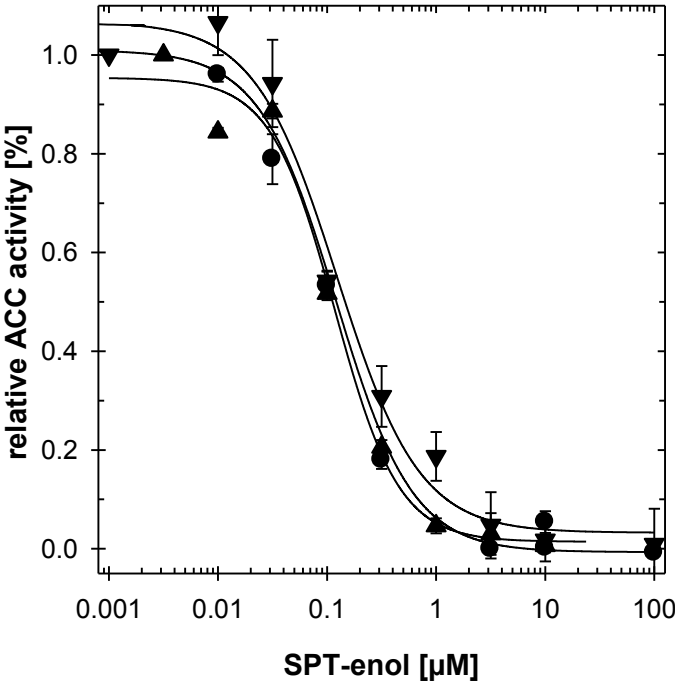


Fig. 5

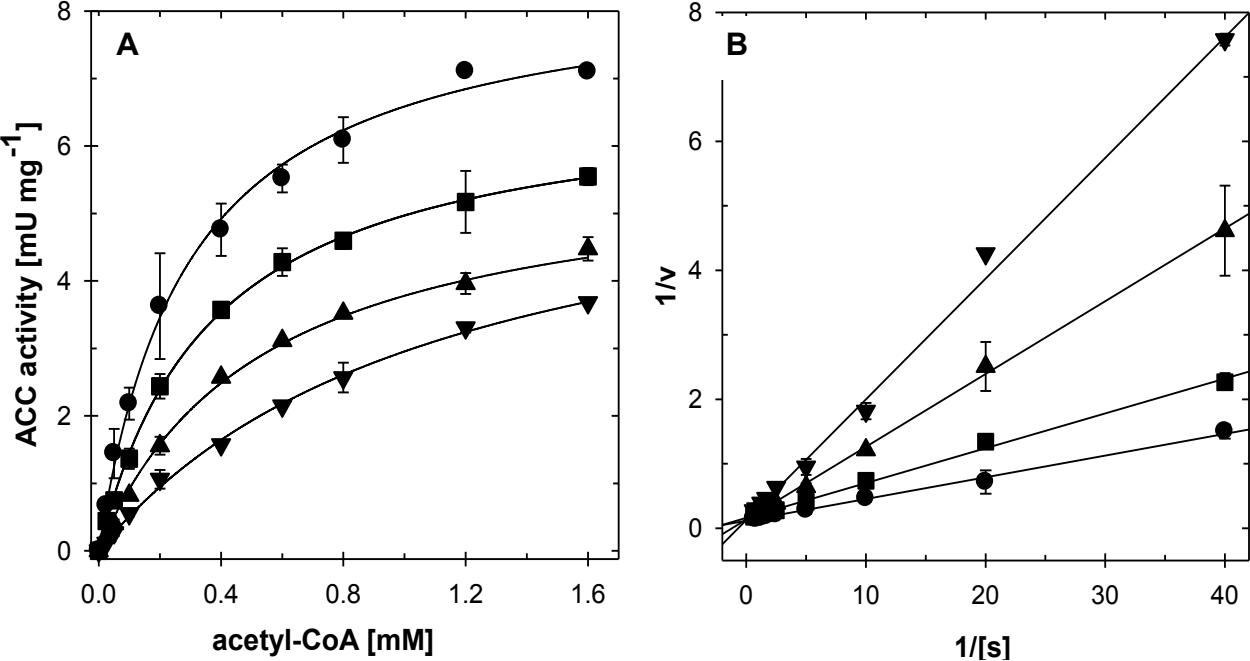


Fig. 6

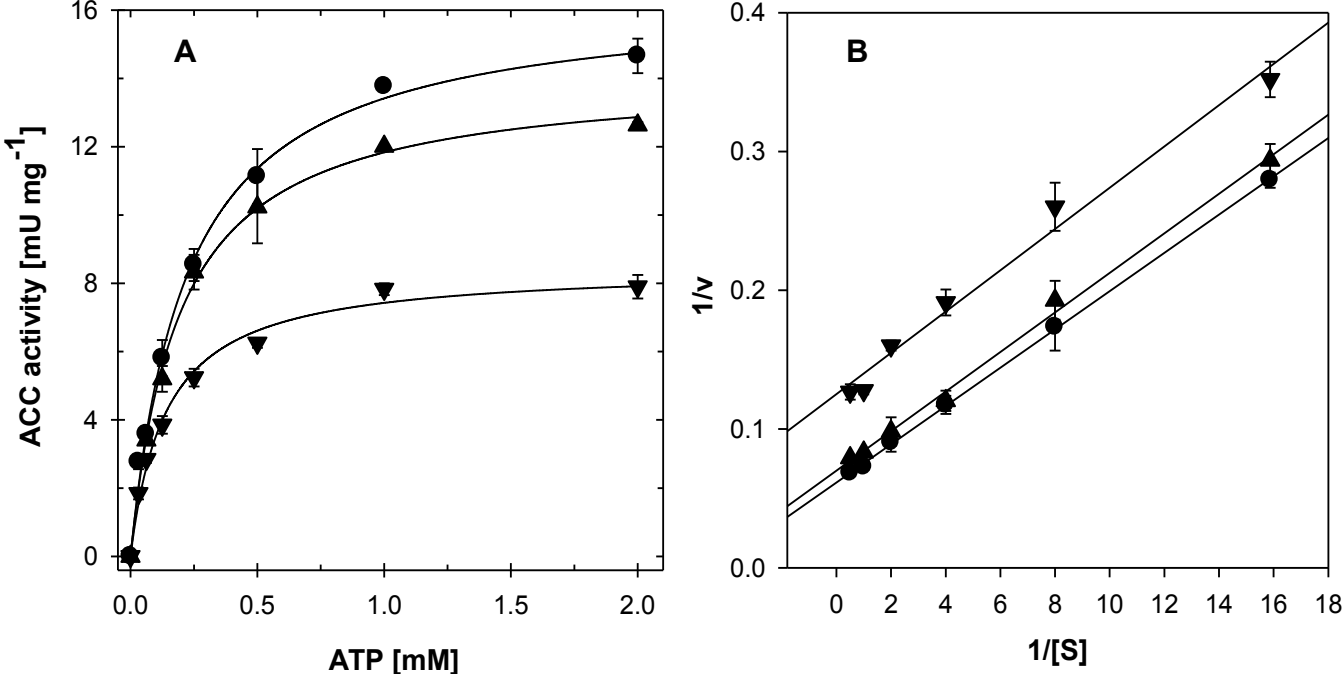


Fig. 7

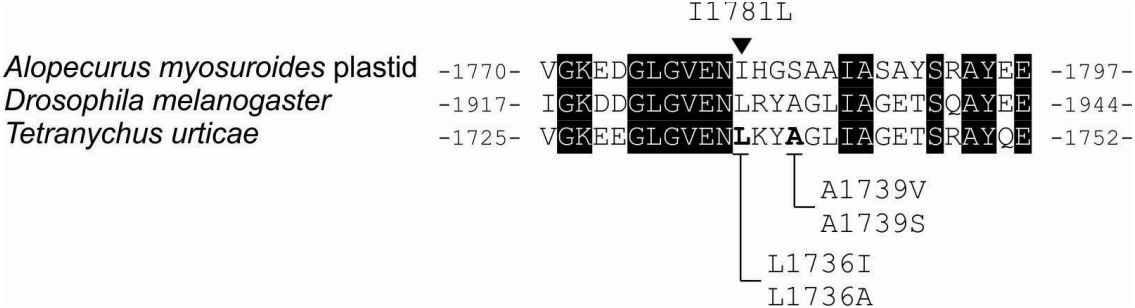


Fig. 8

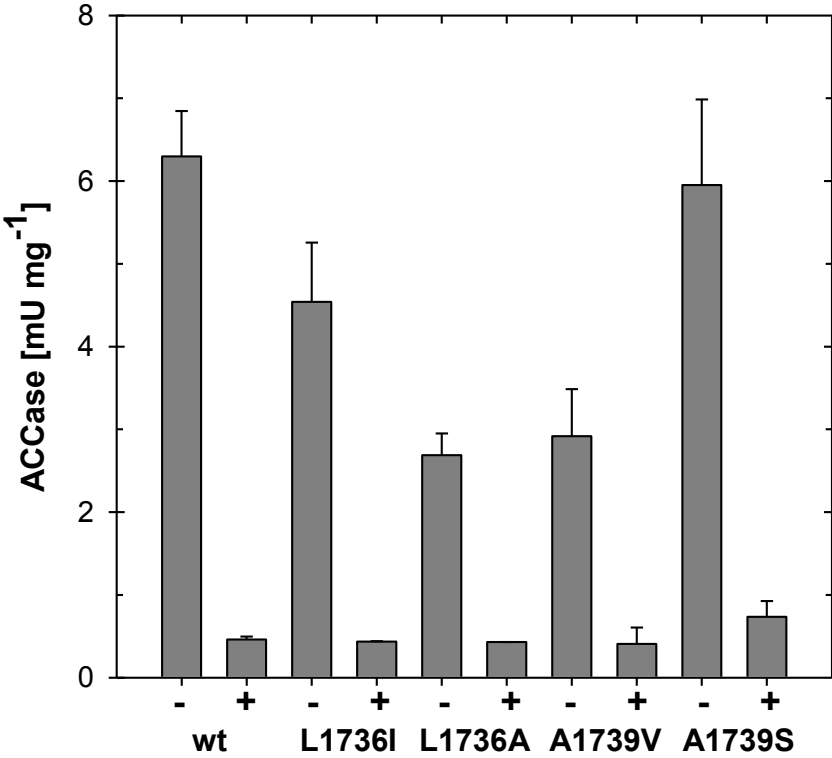


Table 1:

Primers	Sequences (5'–3') ^b
TurACCF3a	ATGAGTGGACCAAATTTATCTTCAC
TuACC-untF3	TTCTATGCCTTTTTGTGTTACCG
TuACC-untR3	TGGTGACATCTCTGATTTTTATGG
TuACC-untR2	TCTGCCCGCTACTAACTTTCA
TurACC-ExpF1	GCGGCCGCGAGTGGACCAAATTTATCTTC
TurACC-ExpR1	TCTAGAACTTTGACGATCCATTTCCA
pFastBacHT-F	CCATCACCATCACGATTACG
pFastBacHT-R	GGACAAACCACA ACTAGAATGC
pUC/M13F	CCCAGTCACGACGTTGTAAAACG
pUC/M13R	AGCGGATAACAATTTCACACAGG

Legends

Fig. 1: Reaction scheme including the two partial reactions of ACC, the ATP-dependent biotin carboxylation, and the carboxyl transfer to acetyl-CoA to form malonyl-CoA.

Fig. 2: Structures of spirotetramat (A) and spirotetramat-enol (B).

Fig. 3: Normalized specific ACC activities, v/V_{\max}^{-1} , as a function of the acetyl-CoA substrate concentration. ACCs were partially purified from *S. frugiperda* (●), *M. persicae* (▲), and *T. urticae* (▼). The corresponding maximum specific activities, V_{\max} , were determined as 7.9 mU mg⁻¹ (*S. frugiperda*), 8.5 mU mg⁻¹ (*M. persicae*), and 18.5 mU mg⁻¹ (*T. urticae*).

Fig. 4: Inhibition of insect and spider mite ACCs by spirotetramat-enol as a function of the concentration. The activities of ACCs from *S. frugiperda* (●), *M. persicae* (▲), and *T. urticae* (▼) were measured at different inhibitor concentrations. IC₅₀ values were calculated from the semi-logarithmic plots by fitting the data to sigmoidal dose-response curves.

Fig. 5: Steady-state kinetic analysis of the insect ACC inhibition by spirotetramat-enol at different acetyl-CoA concentrations. Specific activities of the partially purified *M. persicae* enzyme was measured in the absence (●), or in the presence of SPT-enol at 100 nM (■), 200 nM (▲), and 300 nM (▼), respectively. Kinetic parameters were calculated from direct plots (A), and double-reciprocal plots (B).

Fig. 6: Steady-state kinetic analysis of the insect ACC inhibition by spirotetramat-enol at different ATP concentrations. Specific activities of the partially purified *S. frugiperda* enzyme was measured in the absence (●), or in the presence of SPT-enol at 200 nM (▲), and 300 nM (▼), respectively. Kinetic parameters were calculated from direct plots (A), and double-reciprocal plots (B).

Fig. 7: Alignment of partial CT domain of the ACC of *A. myosuroides* (plastid), the insect *Drosophila melanogaster* and the spider mite *T. urticae*. Conserved residues are shaded in black. The common herbicide resistance mutation in grasses is indicated by a triangle (L1781I), while residues mutated in this study in *T. urticae* ACC are depicted in bold, substitutions are indicated below.

Fig. 8: Specific activities and spirotetramat-enol inhibition of wild-type and mutant ACCs from *T. urticae*. Specific activities were measured in triplicate with partially purified ACCs from baculovirus-infected insect cells expressing either wild-type or mutant ACCs, L1736I, L1736A, A1739V and A1739S. Inhibition by SPT-enol was tested at a fixed inhibitor concentration of 300 nM.

Tab. 1: Primers used in this study

Table 1

Primers	Sequences (5'-3') ^b
TurACCF3a	ATGAGTGGACCAAATTTATCTTCAC
TuACC-untF3	TTCTATGCCTTTTTGTGTTACCG
TuACC-untR3	TGGTGACATCTCTGATTTTTATGG
TuACC-untR2	TCTGCCCGCTACTAACTTTCA
TurACC-ExpF1	GCGGCCGCAGTGGACCAAATTTATCTTC
TurACC-ExpR1	TCTAGAACTTTGACGATCCATTTCCA
pFastBacHT-F	CCATCACCATCACGATTACG
pFastBacHT-R	GGACAAACCACAACCTAGAATGC
pUC/M13F	CCCAGTCACGACGTTGTAAAACG
pUC/M13R	AGCGGATAACAATTCACACAGG

Figure 1
Click here to download high resolution image

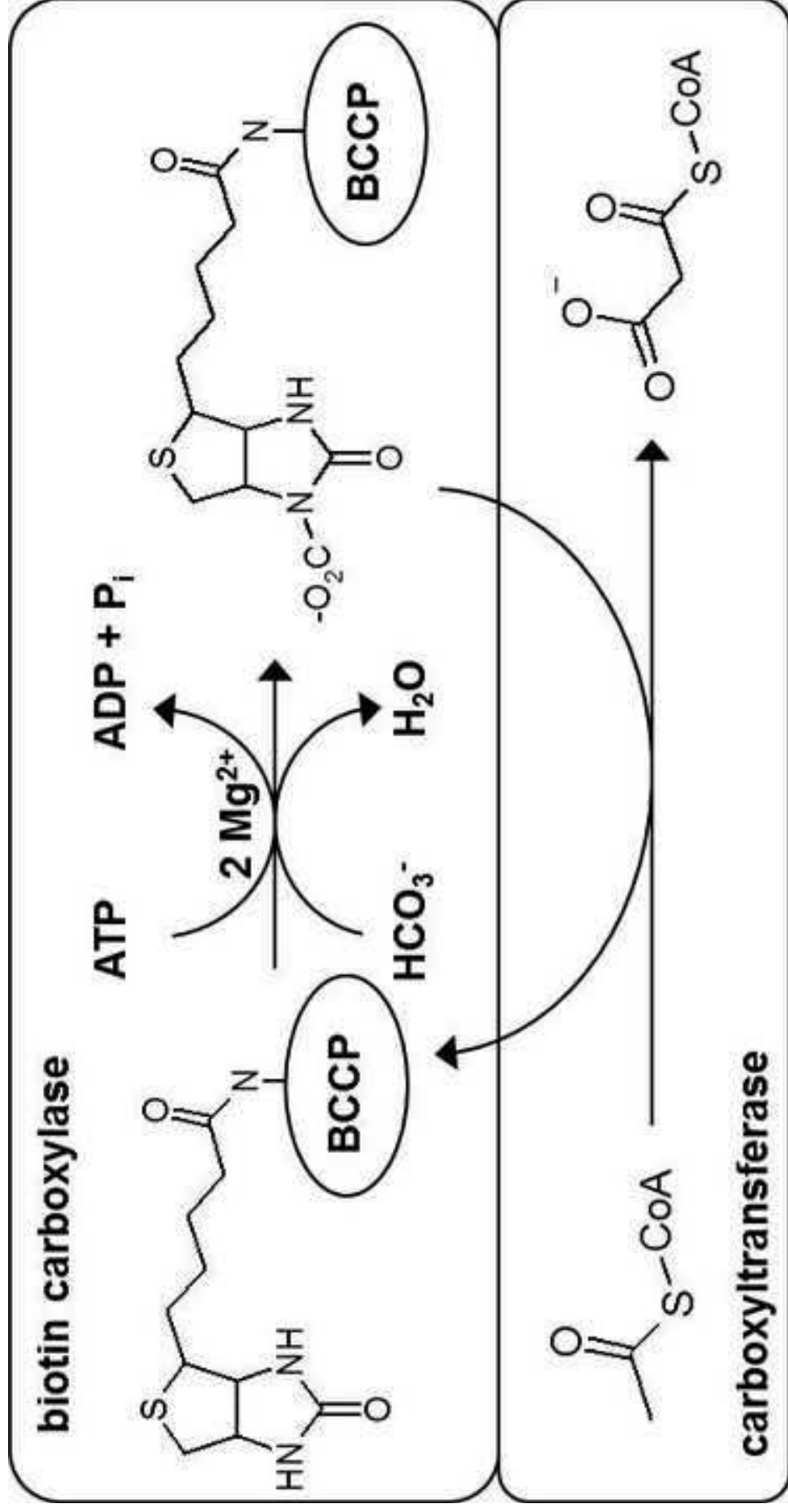


Figure 2
Click here to download high resolution image

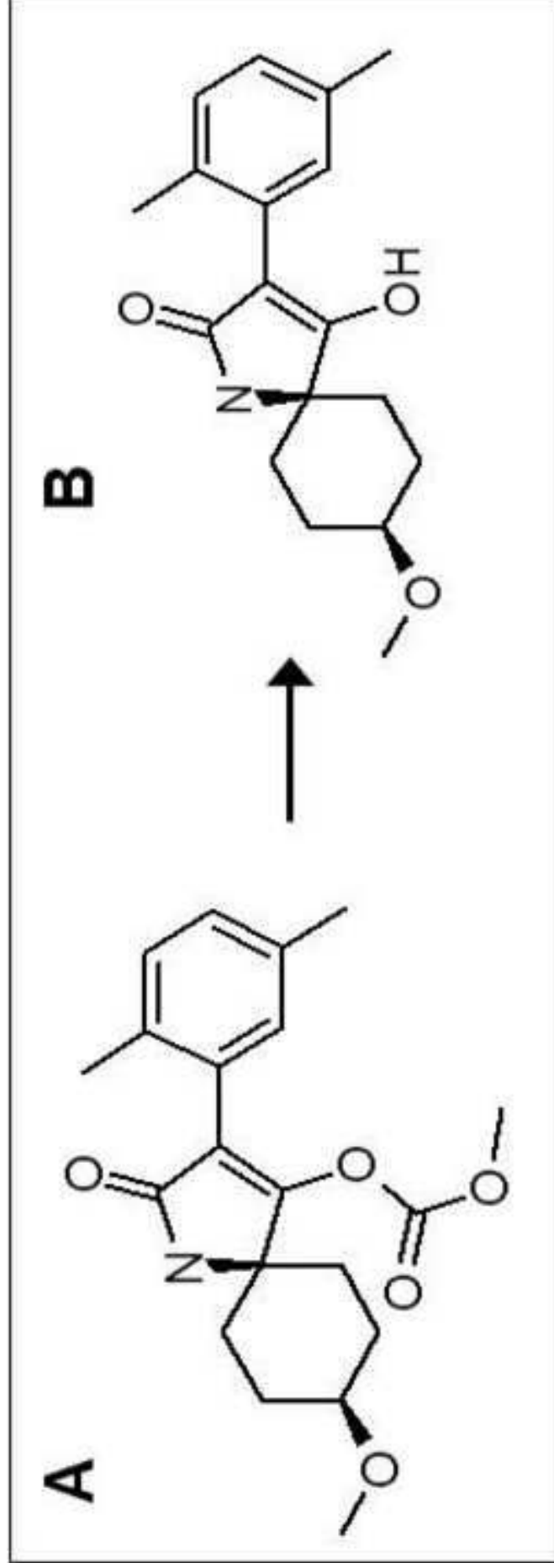


Figure 3
Click here to download high resolution image

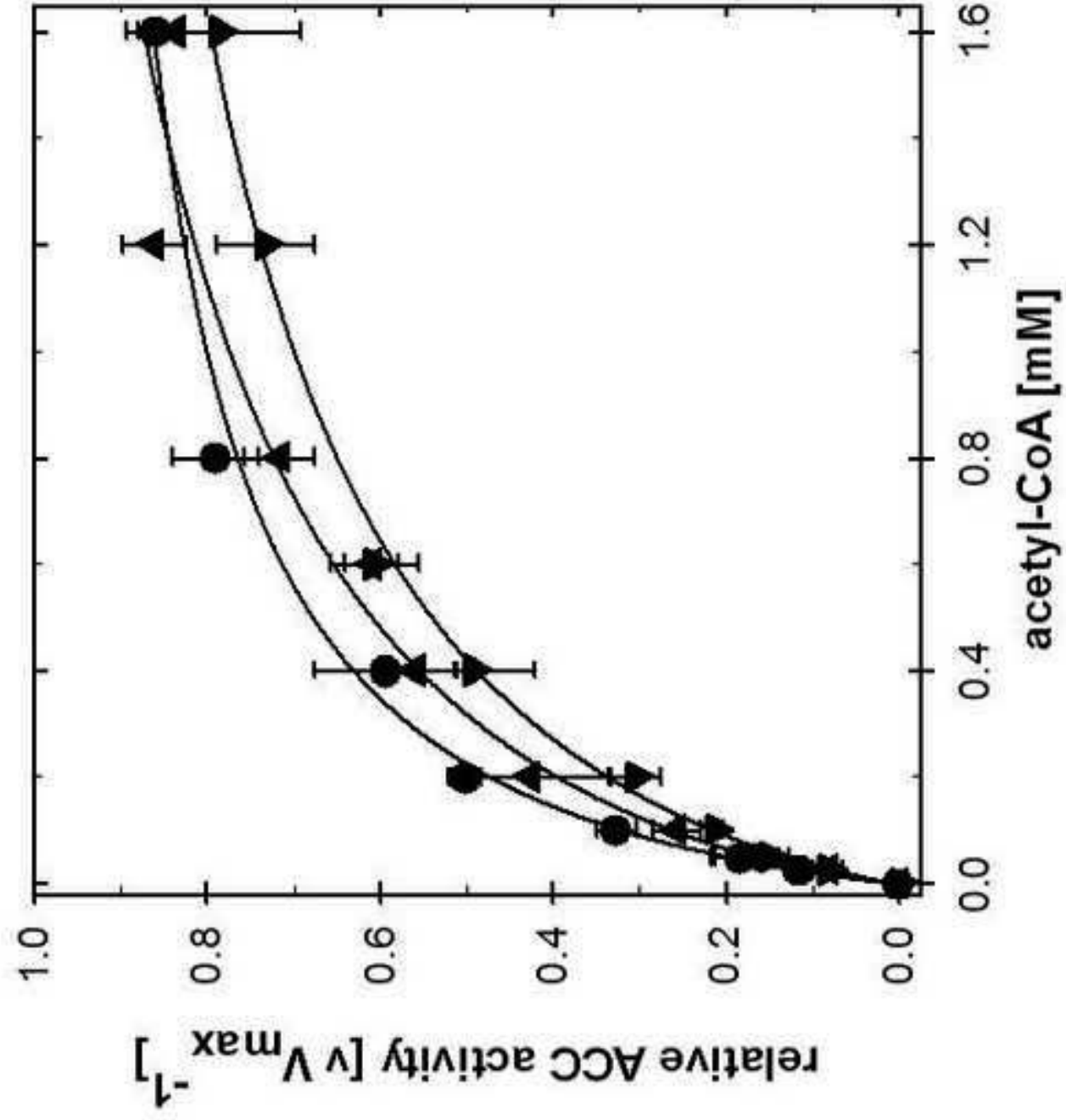


Figure 4
[Click here to download high resolution image](#)

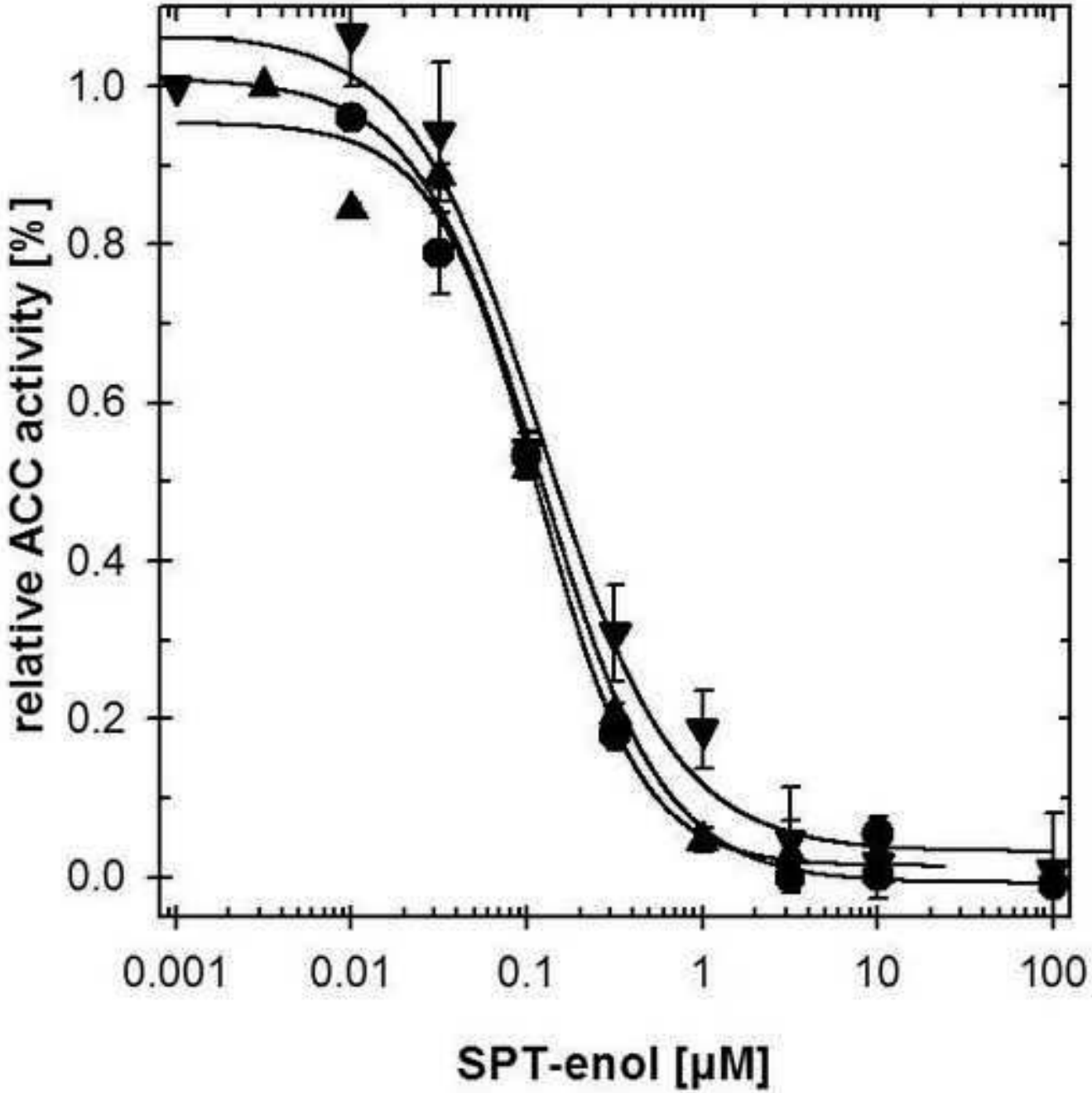


Figure 5
Click here to download high resolution image

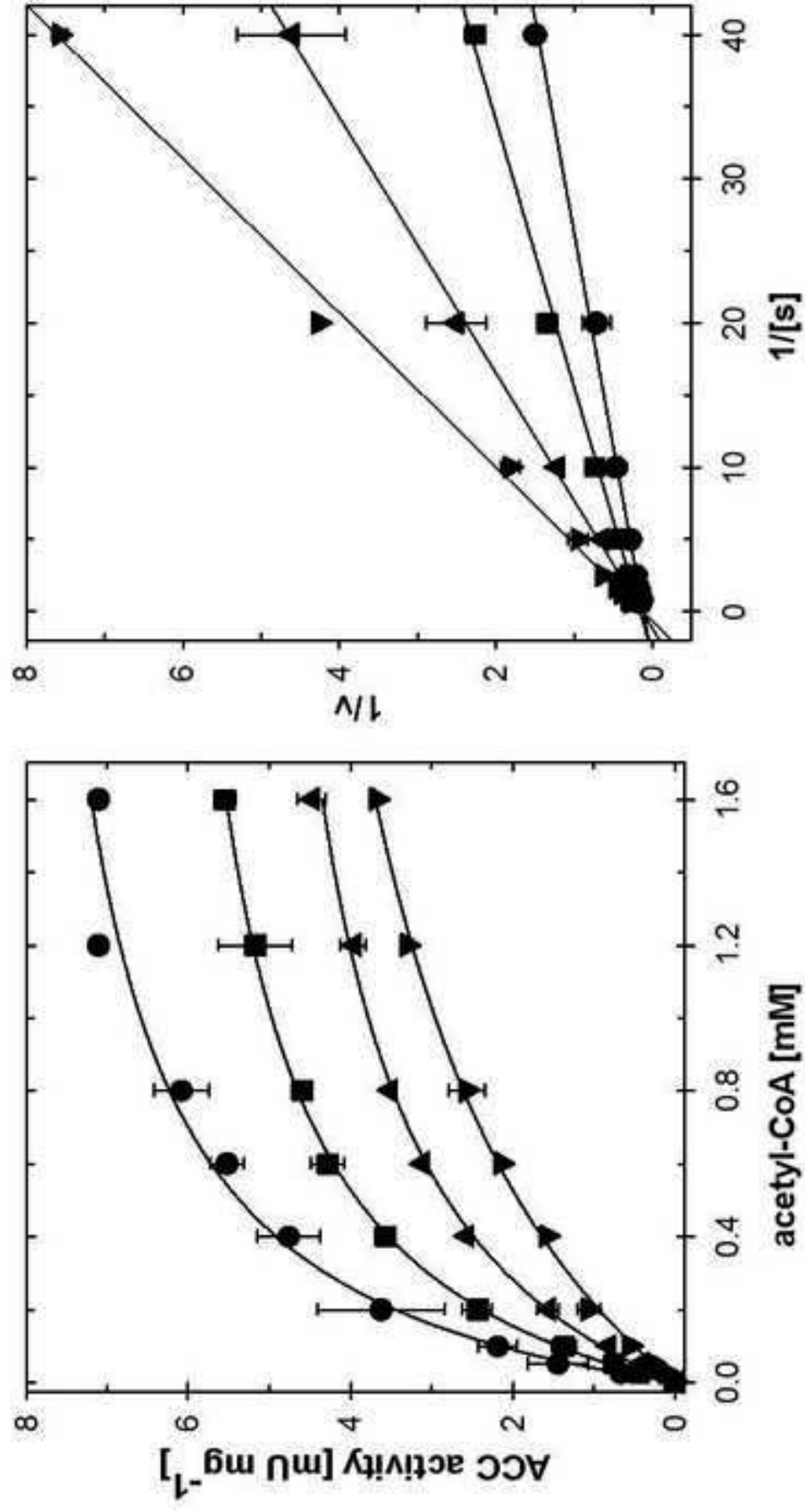


Figure 6
Click here to download high resolution image

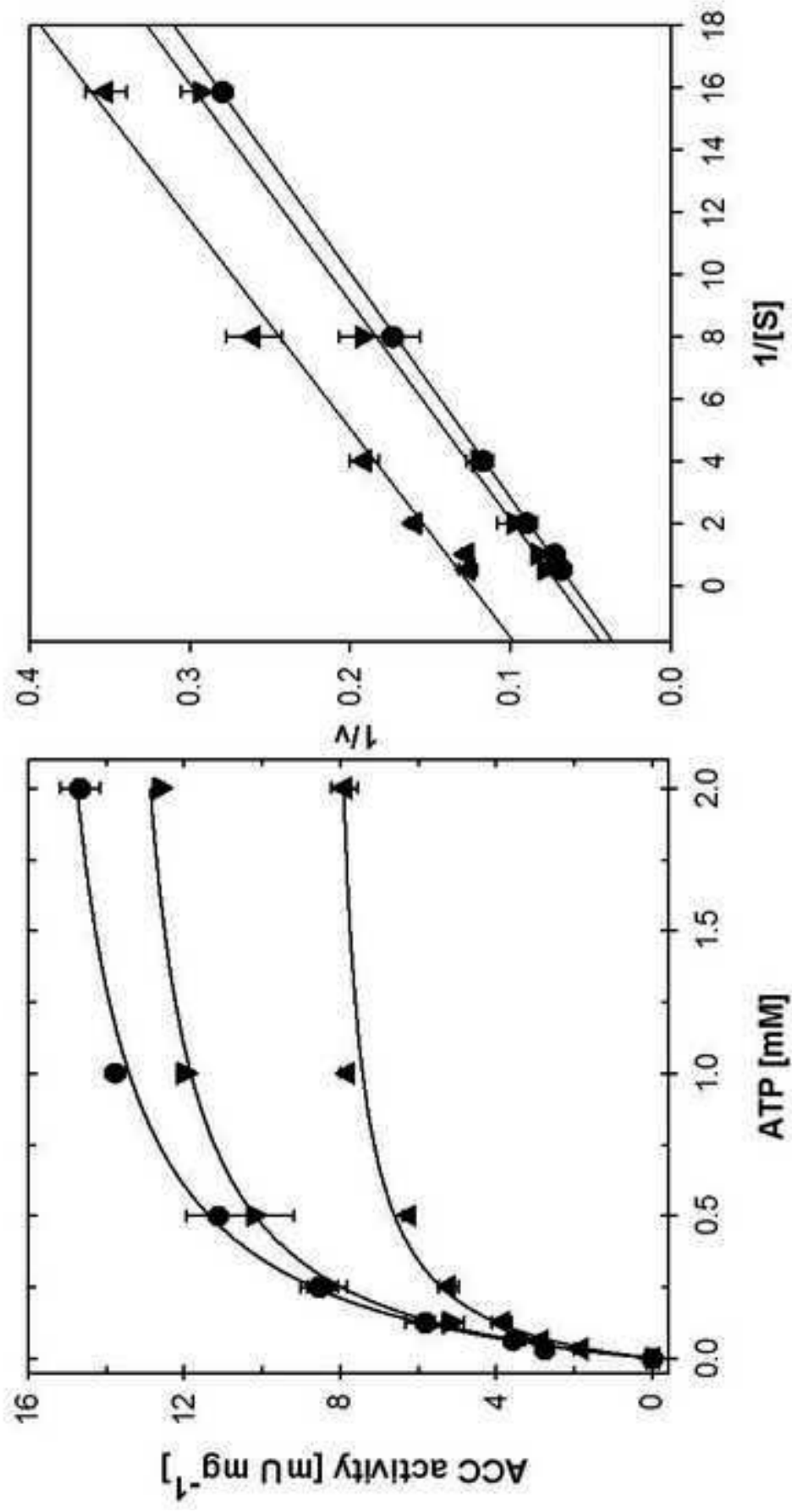


Figure 7
Click here to download high resolution image

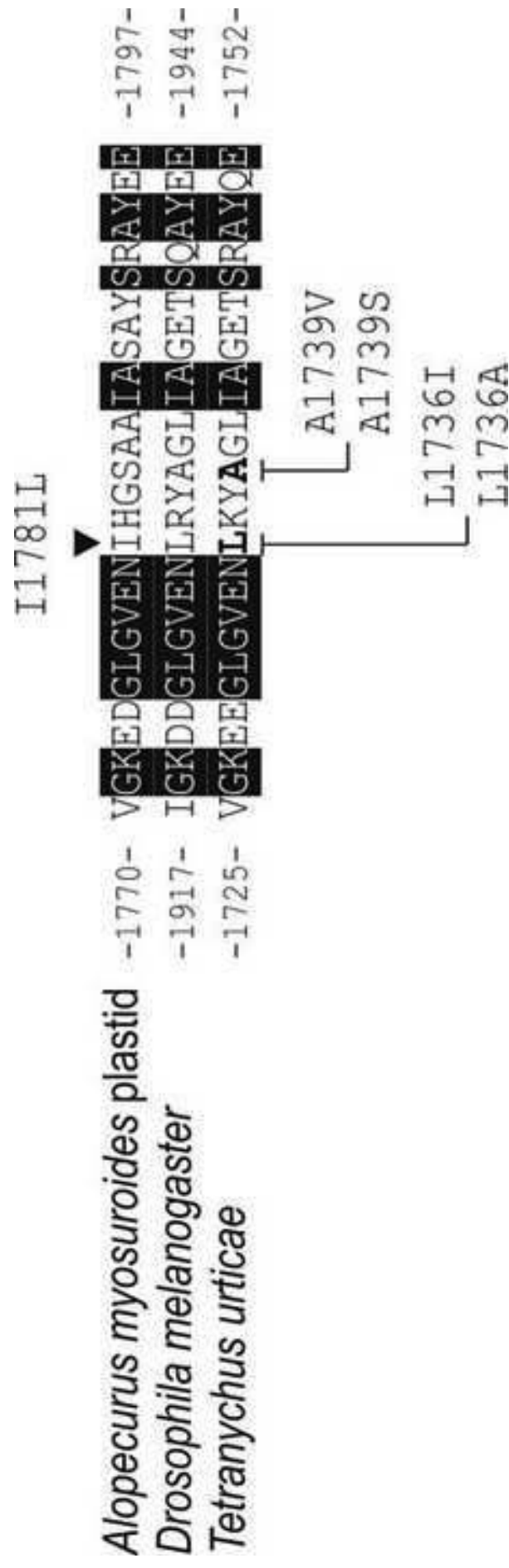


Figure 8
Click here to download high resolution image

